CONTRIBUTION OF WING PLANFORM TO DERIVATIVES OF YAWING MOMENT AND SIDEFORCE DUE TO ROLL RATE AT SUBSONIC SPEEDS, $(N_p)_w$ AND $(Y_p)_w$

1. NOTATION AND UNITS

The derivative notation used is that proposed in ARC R&M 3562 (Hopkin, 1970) and described in Item No. 86021. Coefficients and aeronormalised derivatives are evaluated in aerodynamic body axes with origin at the aircraft centre of gravity and with the wing span as the characteristic length. The derivatives Y_p and N_p are often written as C_{Yp} and C_{np} in other systems of notation, but attention must be paid to the reference dimensions used. In particular, in forming C_{Yp} and C_{np} differentiation of C_Y and C_n may be carried out with respect to $pb/2V$ not pb/V as implied in the Hopkin system. It is also to be noted that a constant datum value of V is employed by Hopkin.

		SI	*British*
A	aspect ratio, b^2/S		
B	Prandtl-Glauert compressibility factor, $\left(1 - M^2 \cos^2\Lambda_{1/4}\right)^{1/2}$		
b	wing span	m	ft
C_D	drag coefficient, $D/\tfrac{1}{2}\rho V^2 S$		
C_D'	viscous drag coefficient, $(C_D - C_L^2/\pi A)$		
C_L	lift coefficient, $L/\tfrac{1}{2}\rho V^2 S$		
C_l	rolling moment coefficient, $\mathscr{L}/\tfrac{1}{2}\rho V^2 S b$		
C_n	wing yawing moment coefficient, $\mathscr{N}/\tfrac{1}{2}\rho V^2 S b$		
C_Y	sideforce coefficient, $Y/\tfrac{1}{2}\rho V^2 S$		
D	drag	N	lbf
F	factor in Equation (5.1)		
L	lift	N	lbf
$\mathscr{L}$	rolling moment	N m	lbf ft
L_p	aeronormalised rolling moment derivative due to roll rate $(\partial \mathscr{L}/\partial p)/\tfrac{1}{2}\rho V S b^2$		
M	free stream Mach number		
$\mathscr{N}$	yawing moment about origin	N m	lbf ft
N_p	aeronormalised yawing moment derivative due to roll-rate $(\partial \mathscr{N}/\partial p)/\tfrac{1}{2}\rho V S b^2$		

p	angular velocity in roll	rad/s	rad/s
S	gross wing area	m^2	ft^2
V	aircraft velocity relative to air	m/s	ft/s
x_{ac}	longitudinal distance rearward from coordinate origin (yawing axis) to wing aerodynamic centre	m	ft
Y	sideforce	N	lbf
Y_p	aeronormalised sideforce derivative due to roll rate $(\partial Y/\partial p)/\frac{1}{2}\rho VSb$		
α	angle of attack	degree	degree
$\Lambda_{\frac{1}{4}}$	quarter-chord sweep of wing planform	degree	degree
λ	ratio of tip chord to centre-line chord (taper ratio)		
ρ	density of air	kg/m^3	$slug/ft^3$

Subscripts

|	
w	denotes wing contribution
M	denotes value in compressible flow
O	denotes value in incompressible flow
$\Lambda_{\frac{1}{4}} = 0$	denotes unswept wing contribution

2. INTRODUCTION

This Item presents a method of estimating the planform contribution to the yawing moment due to roll-rate, $(N_p)_w$, and the sideforce due to roll rate, $(Y_p)_w$, of swept wings at subsonic speeds. The analysis is made for wings without camber, dihedral, or twist, but the effects of sweep angle, aspect ratio, taper ratio and location of yawing axis are considered.

The Item allows the estimation of the initial linear variation of $(N_p)_w$ and $(Y_p)_w$ with lift coefficient, corresponding to fully attached flow, and, for $(N_p)_w$ only, the subsequent non-linear variation with lift coefficient following the onset of flow separation (see Item No. 66033) (Reference 11) for wings with symmetrical sections). The linear components are based largely on lifting-line considerations modified empirically to account for the effects of tip suction (Section 4.2). The non-linear component of $(N_p)_w$ is attributed to the effect of viscous drag which is approximately accounted for on a semi-empirical basis (Section 4.3). Correction factors to the low-speed estimation of $(N_p)_w$ and $(Y_p)_w$ are presented for first order effects of compressible flow (Section 5).

3.   FORCES ON A ROLLING WING

The primary load on a rolling wing with fully attached flow at low angles of attack is made up of a symmetrical load due to angle of attack and an antisymmetrical load due to the rolling velocity. In Derivation 2 the resulting net force at any spanwise wing station is resolved (see Sketch 3.1) into a force, C_1, acting normal to the plane formed by the local resultant velocity, V^*, and its component normal to the quarter-chord line, V_n^*, and a force C_2, acting parallel to V_n^*. Spanwise integration of the components of these forces resolved into the x–y plane multiplied by their appropriate moment arms about the yawing axis, leads to the yawing moment arising from the primary forces. Spanwise integration in the direction of the y-axis leads to the sideforce.

In addition to these primary forces, parts of which are due to a leading-edge suction, there are secondary forces arising from the flow around the wing tips which also contribute to sideforce and yawing moment (see Sketch 3.2 and Derivation 4). The role of the edge forces with regard to the roll-rate derivatives is discussed in some detail in association with lifting-surface theory calculations in Reference 13 and is explained briefly here as follows.
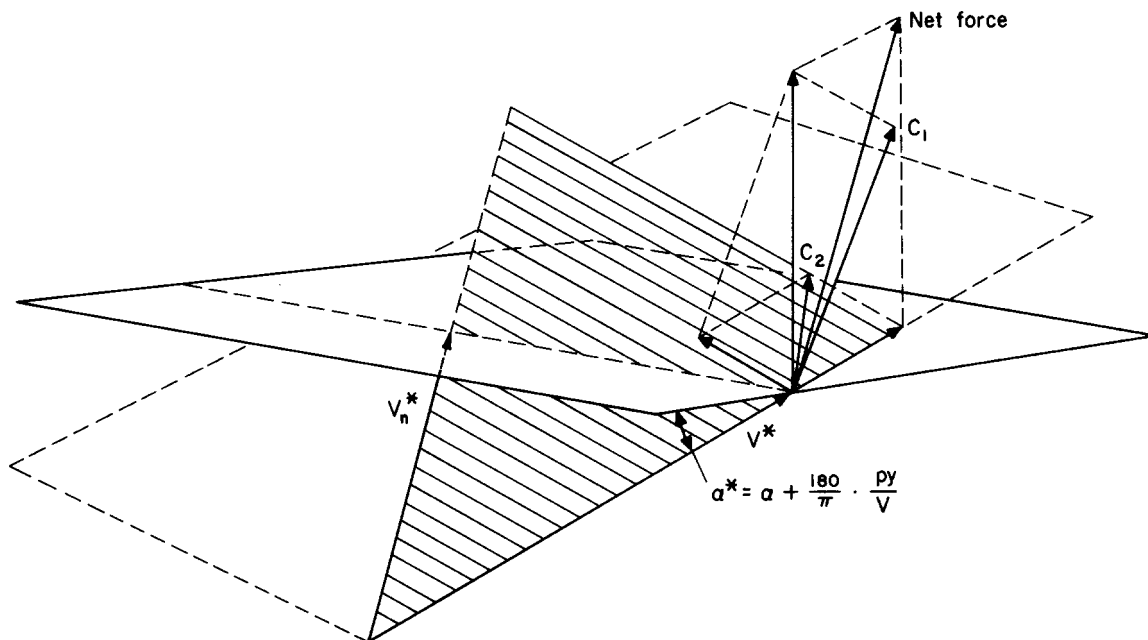
Sketch 3.1   Primary forces on a rolling wing
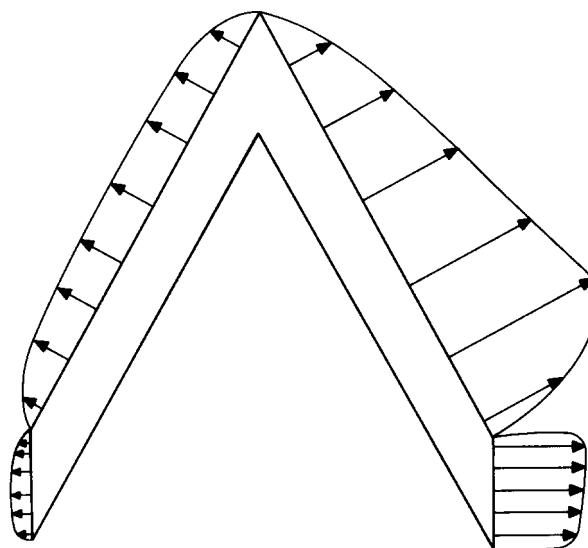
Sketch 3.2 Edge forces on a rolling wing

a. Yawing moment

b. Sideforce
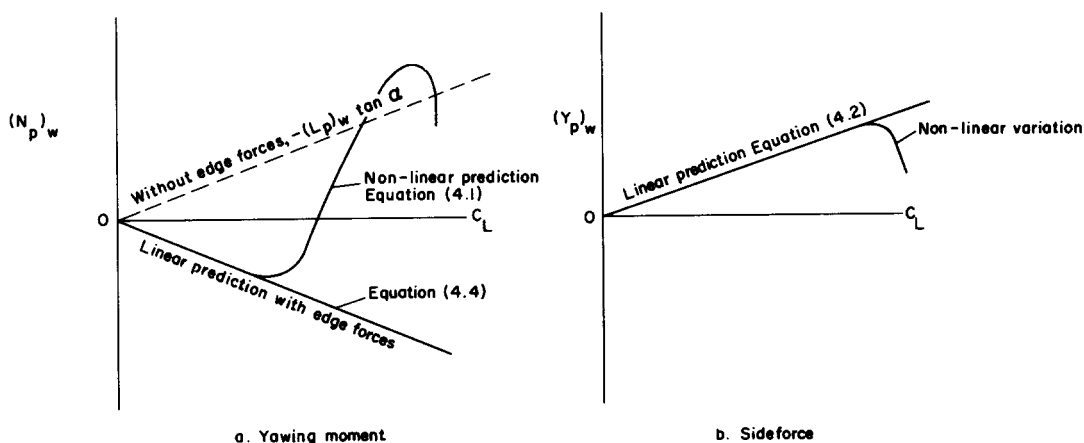
Sketch 3.3 Typical variations of $(N_p)_w$ and $(Y_p)_w$ with C_L

At a sufficiently large angle of attack the flow over the wing will start to separate from the wing surface. For an unswept wing of moderate thickness this will normally occur first at the root trailing-edge for rectangular wings, and at the tip for tapered wings, and will progressively spread to affect the remainder of the wing as the angle of attack increases. For a swept wing the initial separation typically takes the form of a leading-edge vortex starting at the wing tip and spreading inboard as the angle of attack increases.

The main effect of such separations on the forces acting on a rolling wing lies in the progressive collapse of the leading-edge and tip suction contributions as the angle of attack increases. The resultant effect is a rapid reduction in the magnitudes of the sideforce and yawing moment and their derivatives with respect to roll rate (see Sketch 3.3). There comes a point at which the progressive loss of the edge forces will normally result in a change in sign of the yawing moment derivative. A knowledge of the lift coefficient at which the change in sign of $(N_p)_w$ occurs is of particular importance in assessing various aspects of the lateral stability of an aircraft and can be deduced by means of this Item.

As the separated flow spreads over most of the wing at the approach to the stall, the suction peaks and all the edge forces virtually disappear and the resultant force then acts normal to the planform of the wing. The yawing moment derivative in these conditions approaches $-(L_p)_w \tan\alpha$, the theoretical contribution from the roll-damping derivative (see Sketch 3.3a, Derivation 6 and Reference 13).

The rapid spread of separation at high angles of attack is reflected in the rate of change of viscous drag coefficient, C_D', with angle of attack. This is employed in Derivation 4 as a correlating parameter for the changes in $(N_p)_w$ due to separation effects. The very large values of $dC_D'/d\alpha$ near the stall can, and often do, lead to the experimental values of $(N_p)_w$ "overshooting" the theoretical limit without edge forces before they finally decrease (see Sketch 3.3a).

4. INCOMPRESSIBLE FLOW

4.1 General

The wing planform contribution due to the derivatives of yawing moment due to roll rate, $(N_p)_w$, and sideforce due to roll rate, $(Y_p)_w$ at low speeds, are given by the following semi-empirical equations which apply to wings without camber, dihedral or twist,

$$[(N_p)_w]_O = C_L \frac{A+4}{A+4\cos\Lambda_{1/4}} \left[1 + 6\left(1 + \frac{\cos\Lambda_{1/4}}{A}\right)\left(\frac{x_{ac}}{b}\tan\Lambda_{1/4} + \frac{\tan^2\Lambda_{1/4}}{12}\right)\right]\left[\frac{(N_p)_w}{C_L}\right]_{O,\,\Lambda_{1/4}=0}$$

$$- \frac{C_L}{4A(1+\lambda)}\left(\frac{2+\lambda}{3}\tan\Lambda_{1/4} + \frac{\lambda}{A}\right) - \frac{C_L}{2A}\frac{x_{ac}}{b} + \frac{(\Delta N_p)_w}{(dC_D'/d\alpha)}\frac{dC_D'}{d\alpha}\,, \qquad (4.1)$$

$$[(Y_p)_w]_O = \frac{C_L}{2}\left(\frac{A+\cos\Lambda_{1/4}}{A+4\cos\Lambda_{1/4}}\right)\tan\Lambda_{1/4} + \frac{C_L}{2A}\,. \qquad (4.2)$$

4.2 Linear Contribution

4.2.1 Yawing moment due to roll rate, $(N_p)_w$

In Equation (4.1) the first three terms relate to the linear contribution. The first term, which may be written as

$$\left[\frac{(N_p)_w}{C_L}\right]_O = \frac{A+4}{A+4\cos\Lambda_{1/4}}\left[1 + 6\left(1 + \frac{\cos\Lambda_{1/4}}{A}\right)\left(\frac{x_{ac}}{b}\tan\Lambda_{1/4} + \frac{\tan^2\Lambda_{1/4}}{12}\right)\right]\left[\frac{(N_p)_w}{C_L}\right]_{O,\,\Lambda_{1/4}=0}\,, \qquad (4.3)$$

was developed in Derivation 2 from strip theory and simple lifting-line considerations. It arises from interactions between symmetrical forces due to incidence and anti-symmetrical forces due to roll rate (see Section 3). The wing sweep factor was developed for untapered wings but the effects of taper are assumed to be accounted for by using the sweepback relating to the quarter-chord line.

The quantity for unswept wings in Equation (4.3) (*i.e.* $[(N_p)_w/C_L]_{O,\,\Lambda_{1/4}=0}$) has been calculated theoretically in Derivation 2 using data from Derivation 1 to allow for the small effect of taper.

The second and third terms relate to the effect of tip suction and were derived in Derivation 4 for untapered wings and modified in Derivation 6 to account for the effect of taper. The indications from experimental data (Derivation 5) are that wing taper has a minor effect on $(N_p)_w$ provided the quarter-chord sweep angle is used. With this assumption Figure 1 presents data for the linear contribution to $(N_p)_w$, obtained from the first three terms in Equation (4.1) with $\lambda = 1$, *i.e.*

$$\left[\frac{(N_p)_w}{C_L}\right]_O = \frac{A+4}{A+4\cos\Lambda_{1/4}}\left[1 + 6\left(1 + \frac{\cos\Lambda_{1/4}}{A}\right)\left(\frac{x_{ac}}{b}\tan\Lambda_{1/4} + \frac{\tan^2\Lambda_{1/4}}{12}\right)\right]\left[\frac{(N_p)_w}{C_L}\right]_{O,\Lambda_{1/4}=0}$$

$$- \frac{1}{8A}\left(\tan\Lambda_{1/4} + \frac{1}{A}\right) - \frac{1}{2A}\frac{x_{ac}}{b}. \qquad (4.4)$$

Figure 1 covers a range of sweep angles up to $60°$ and aspect ratios from 2 to 12 for fixed values of $x_{ac}/b = 0.0$, 0.1 and 0.2. The position of the aerodynamic centre to be used in the calculation of x_{ac}/b may be found from Item No. 70011 (Reference 12).

4.2.2 Sideforce due to roll rate, $(Y_p)_w$

The first term of Equation (4.2), which may be written as

$$\left[\frac{(Y_p)_w}{C_L}\right]_O = \frac{A+\cos\Lambda_{1/4}}{A+4\cos\Lambda_{1/4}}\frac{\tan\Lambda_{1/4}}{2},$$

was developed in Derivation 2 from strip theory and simple lifting-line considerations. The equation was originally developed for untapered wings but the effects of taper are assumed to be accounted for by using the sweepback relating to the quarter-chord line. The second term in Equation (4.2) relates to the effect of tip suction. It was derived empirically in Derivation 4 as the zero sweep contribution for untapered wings, and is considered here to apply to tapered wings by referring the sweepback to the quarter-chord line, *i.e.*

$$\left[\frac{(Y_p)_w}{C_L}\right]_{\Lambda_{1/4}=0} = \frac{1}{2A}.$$

It should be noted that this term has been used in Derivation 4 to derive the tip suction terms in Equation (4.1) for $(N_p)_w$.

Figure 2 gives the ratio $(Y_p)_w/C_L$ in incompressible flow for a range of sweep angles up to $60°$ and aspect ratios from 2 to 12, obtained from

$$\left[\frac{(Y_p)_w}{C_L}\right]_O = \frac{1}{2}\left(\frac{A+\cos\Lambda_{1/4}}{A+4\cos\Lambda_{1/4}}\right)\tan\Lambda_{1/4} + \frac{1}{2A}. \qquad (4.5)$$

4.3 Non-linear Contribution to $(N_p)_w$

The fourth term in Equation (4.1) relates to the non-linear contribution to $(N_p)_w$, *i.e.*

$$\frac{(\Delta N_p)_w}{(\mathrm{d}\,C'_D\,/\mathrm{d}\alpha)}\frac{\mathrm{d}C'_D}{\mathrm{d}\alpha}\,.\tag{4.6}$$

It arises from the effects of flow separations over the wing at moderate to high lift coefficients. Derivation 4 suggests that the non-linear increment in $(N_p)_w$ can be correlated in terms of the rate of change of viscous drag coefficient with angle of attack, *i.e.* $\mathrm{d}C'_D/\mathrm{d}\alpha$, where C'_D is assumed to be given by $C_D - C_L^2/\pi A$. The result of the analysis of Derivation 4, modified in Derivation 7 to extract a wing sweep effect, is shown in Figure 3. It should be noted that in order to calculate $(\Delta N_p)_w$ via Figure 3, it is necessary to have drag data for the wing under consideration at sufficiently close intervals in α for a satisfactory determination of $\mathrm{d}C'_D/\mathrm{d}\alpha$ to be made, since $(\Delta N_p)_w$ is very sensitive to changes in $\mathrm{d}C'_D/\mathrm{d}\alpha$.

5. COMPRESSIBLE FLOW

Derivation 3 gives an approximate method for determining the first order effects of compressible flow. Equation (4.4) together with the Prandtl-Glauert rule gives the correction factor due to compressibility for $(N_p)_w$ as

$$\frac{[(N_p)_w/C_L]_M}{[(N_p)_w/C_L]_O}=\frac{A+4\cos\Lambda_{\frac14}}{AB+4\cos\Lambda_{\frac14}}\cdot\frac{AB+6F(AB+\cos\Lambda_{\frac14})}{A+6F(A+\cos\Lambda_{\frac14})}\,,\tag{5.1}$$

where $B=(1-M^2\cos^2\Lambda_{\frac14})^{\frac12}$ and $F=\left(\dfrac{x_{ac}}{b}\tan\Lambda_{\frac14}+\dfrac{\tan^2\Lambda_{\frac14}}{12}\right)$.

The parameter x_{ac}/b has a negligible effect on the correction equation and may be assumed to be zero in Equation (5.1), *i.e.*

$$\frac{[(N_p)_w/C_L]_M}{[(N_p)_w/C_L]_O}=\frac{A+4\cos\Lambda_{\frac14}}{AB+4\cos\Lambda_{\frac14}}\cdot\frac{AB+\frac12(AB+\cos\Lambda_{\frac14})\tan^2\Lambda_{\frac14}}{A+\frac12(A+\cos\Lambda_{\frac14})\tan^2\Lambda_{\frac14}}\,.\tag{5.2}$$

Similarly, Derivation 3 gives the correction factor due to compressibility for the sideforce derivative, $(Y_p)_w$, as

$$\frac{[(Y_p)_w/C_L]_M}{[(Y_p)_w/C_L]_O}=\frac{A+4\cos\Lambda_{\frac14}}{AB+4\cos\Lambda_{\frac14}}\cdot\frac{AB+\cos\Lambda_{\frac14}}{A+\cos\Lambda_{\frac14}}\,.\tag{5.3}$$

Figures 4 and 5 give the compressibility corrections in carpets of Mach number and quarter-chord sweep angle obtained from Equations (5.2) and (5.3) for a range of aspect ratios. It should be noted that although the data were derived from a method neglecting tip suction effects, it may be assumed that Figures 4 and 5 apply to the whole of the linear contribution at least. In the absence of further information the data of Figure 4 may also be tentatively applied to the non-linear component. The data of Figures 4 and 5 apply to Mach numbers up to that at which the aerodynamic characteristics start to change rapidly. This restriction means that in practice the actual effects of Mach number on $(N_p)_w$ and $(Y_p)_w$ will be comparatively small.

6. ACCURACY AND APPLICABILITY

6.1 Accuracy

6.1.1 $(N_p)_w$

Values of the yawing moment derivative due to roll rate, $(N_p)_w$, from the experimental data of Derivations 4 to 6 and References 8 to 10 were compared with predictions firstly in the regime where $(N_p)_w$ varies linearly with lift coefficient and secondly over the complete lift coefficient range tested, up to the stall in some cases.

In the linear regime 90 per cent of the experimental data for $(N_p)_w$ were predicted to within ± 0.005 by means of Figure 1 (Equation (4.4)) with Figure 4 (Equation (5.2)) for compressibility effects.

With the inclusion of non-linear conditions 80 per cent of the experimental data were predicted to within ± 0.01 and 64 per cent to within ± 0.005 by means of Figures 1, 3 and 4 (Equation (4.4) plus Equation (4.6) with Equation (5.2) for compressibility effects) together with wind-tunnel lift and drag data presented in each report for the wing planforms considered.

6.1.2 $(Y_p)_w$

Values of sideforce derivative due to roll rate, $(Y_p)_w$, from experimental data of Derivations 4 to 6 and References 8 to 10 were compared with predictions in the regime where $(Y_p)_w$ varies linearly with lift coefficient. Using Figure 2 (Equation (4.5)) with Figure 5 (Equation (5.3)) for compressibility effects, 90 per cent of the experimental data for $(Y_p)_w$ were predicted to within ± 0.05.

6.2 Applicability

The methods presented in this Item apply to wing planforms without camber, dihedral or twist, in the "clean" condition, *i.e.* with high-lift devices retracted. The methods have been developed from data for untapered wings $(\lambda = 1)$, although the small effect of taper can be accounted for, in the linear contribution to $(N_p)_w$ at least, using Equation (4.1). The methods of Section 4.2 apply to wing planforms in the region where the rates of change of yawing moment with roll rate, $(N_p)_w$, and sideforce with roll rate, $(Y_p)_w$, are essentially linear with lift coefficient, C_L. Equations (4.4) and (4.5) are therefore suitable for use at the project design stage. Experimental evidence for $(N_p)_w$ and $(Y_p)_w$ however, invariably shows a non-linear dependence on C_L at moderate to high lift coefficients. The non-linear dependence of $(N_p)_w$ can be accounted for as detailed in Section 4.3 but the method is only usable if adequate data for lift and drag are available for the wing planform considered.

Most of the experimental data studied were for low subsonic Mach numbers but a few data were obtained for Mach numbers up to 0.70 and these confirmed the use of Equations (5.2) and (5.3) to account for the effects of compressible flow on $(N_p)_w$ and $(Y_p)_w$, respectively.

Table 6.1 shows the ranges of the experimental data studied in the preparation of this Item and the methods should be used with caution for wing planforms having geometric parameters outside these ranges, with the exception of higher aspect ratios.

TABLE 6.1 Range of Experimental Data

Parameter	Range
A	1.34 to 5.16
λ	0.25 to 1.0
$\Lambda_{\frac{1}{4}}$	0 to 60°
M	0.13 to 0.70

For the experimental data considered, the yawing axis was close enough to the aerodynamic centre of the wing for the assumption $x_{ac} = 0$ to be made.

7. DERIVATION AND REFERENCES

7.1 Derivation

The Derivation lists selected sources that have assisted in the preparation of this Item.

1. PEARSON, H.A.
    JONES, R.T.
    Theoretical stability and control characteristics of wings with various amounts of taper and twist. NACA Rep. 635, 1938.

2. TOLL, T.A.
    QUEIJO, M.J.
    Approximate relations and charts for low-speed stability derivatives of swept wings. NACA tech. Note 1581, 1948.

3. FISHER, L.R.
    Approximate corrections for the effects of compressibility on the subsonic stability derivatives of swept wings. NACA tech. Note 1854, 1949.

4. GOODMAN, A.
    FISHER, L.R.
    Investigation at low speeds of the effect of aspect ratio and sweep on rolling stability derivatives of untapered wings. NACA Rep. 968, 1950.

5. BREWER, J.D.
    FISHER, L.R.
    Effect of taper ratio on the low-speed rolling stability derivatives of swept and unswept wings of aspect ratio 2.61. NACA tech. Note 2555, 1951.

6. WIGGINS, J.W.
    Wind-tunnel investigation of effect of sweep on rolling derivatives at angles of attack up to 13° and at high subsonic Mach numbers including a semi-empirical method of estimating the rolling derivatives. NACA tech. Note 4185, 1958.

7. WOLOWICZ, C.H.
    YANCEY, R.B.
    Lateral directional aerodynamic characteristics of light, twin-engine, propeller-driven airplanes. NASA tech. Note D-6946, 1972.

7.2 References

The References list selected sources of information supplementary to that given in this Item.

8.	LETKO, W. RILEY, D.R.	Effect of an unswept wing on the contribution of unswept-tail configurations to the low-speed static- and rolling-stability derivatives of a midwing airplane model. NACA tech. Note 2175, 1950.
9.	FISHER, L.R. MICHAEL, W.H.	An investigation of the effect of vertical-fin location and area on low-speed lateral stability derivatives of a semi-tailless airplane model. NACA RM L51A10 (TIL 2655), 1951.
10.	WOLHART, W.D.	Influence of wing and fuselage on the vertical tail contribution to the low-speed rolling derivatives of midwing airplane models with 45° sweptback surfaces. NACA tech. Note 2587, 1951.
11.	ESDU	Boundaries of linear characteristics of plane, symmetrical section wings at subcritical Mach numbers. Item No. 66033, Engineering Sciences Data Unit, London, October 1966.
12.	ESDU	Lift-curve slope and aerodynamic centre position of wings in inviscid subsonic flow. Item No. 70011, Engineering Sciences Data Unit, London, July 1970.
13.	GARNER, H.C.	On the application of subsonic wing-theory to edge forces and roll-rate derivatives. RAE tech. Rep. 73030, 1973.

8. EXAMPLES

8.1 Example 1

It is required to estimate the planform contributions to N_p and Y_p for a wing, with geometrical parameters $A = 6$ and $\Lambda_{1/4} = 30°$, with fully attached flow at a lift coefficient of 0.15 and a Mach number of 0.7. The yawing axis is located at the aerodynamic centre of the wing (*i.e.* $x_{ac}/b = 0$).

From Figures 1 and 2 with $A = 6$ and $\Lambda_{1/4} = 30°$, for incompressible flow,

$$\left[\frac{(N_p)_w}{C_L}\right]_O = -0.047 \quad \text{and} \quad \left[\frac{(Y_p)_w}{C_L}\right]_O = 0.293 \,.$$

From Figures 4 and 5 with $\Lambda_{1/4} = 30°$ and $M = 0.70$, the correction factors for compressible flow are

$$\frac{[(N_p)_w/C_L]_M}{[(N_p)_w/C_L]_O} = 0.919 \quad \text{and} \quad \frac{[(Y_p)_w/C_L]_M}{[(Y_p)_w/C_L]_O} = 0.944 \,.$$

Therefore, for compressible flow, at $M = 0.7$,

$$\left[\frac{(N_p)_w}{C_L}\right]_M = -0.047 \times 0.919 = -0.0432$$

and

$$\left[\frac{(Y_p)_w}{C_L}\right]_M = 0.293 \times 0.944 = 0.277 \,.$$

Thus for $C_L = 0.15$, $[(N_p)_w]_M = -0.0432 \times 0.15 = -0.0065$

and

$$[(Y_p)_w]_M = 0.277 \times 0.15 = 0.0416 \approx 0.042 \,.$$

8.2 Example 2

It is required to estimate the planform contribution to N_p for a wing planform in incompressible flow over a range of lift coefficients including conditions for which vortex separation occurs on the wing leading edge. Data for the change of viscous drag coefficient with incidence for the lift coefficient range considered is supplied (Table 8.1). The geometrical parameters of the wing planform are $A = 2.61$ and $\Lambda_{1/4} = 60°$. The yawing axis is located at the aerodynamic centre of the wing (*i.e.* $x_{ac}/b = 0$).

TABLE 8.1

C_L	0	0.1	0.2	0.3	0.4	0.5	0.6	0.7	0.8
$\dfrac{dC_D'}{d\alpha}$ (per degree)	0	0	0.0006	0.0014	0.0022	0.0103	0.014	0.016	0.016

For $A = 2.61$ and $\Lambda_{1/4} = 60°$ from Figure 1, for incompressible flow, for the linear contribution

$$\left[\frac{(N_p)_w}{C_L}\right]_O = -0.154 .$$

From Figure 3, for the non-linear increment,

$$(\Delta N_p)_w / (d\,C_D'/d\alpha) = 10 \text{ degrees.}$$

The total planform contribution to $(N_p)_w$ from Equation (4.4) plus Equation (4.6) is,

$$(N_p)_w = C_L\left[\frac{(N_p)_w}{C_L}\right]_O + \frac{(\Delta N_p)_w}{(d\,C_D'/d\alpha)}\frac{dC_D'}{d\alpha} ,$$

i.e.
$$(N_p)_w = C_L(-0.154) + 10 \times \frac{dC_D'}{d\alpha} .$$

The calculation for $C_L = 0.5$ will be carried out as an example. From Table 8.1 for $C_L = 0.5$, $dC_D'/d\alpha = 0.0103$ per degree, so that $(N_p)_w = 0.5(-0.154) + 10(0.0103) = 0.026$. The results of the calculations for the other values of C_L are given in Table 8.2 and illustrated graphically in Sketch 8.1.

TABLE 8.2

C_L	0	0.1	0.2	0.3	0.4	0.5	0.6	0.7	0.8
$(N_p)_w$	0	–0.015	–0.025	–0.032	–0.040	+0.026	+0.048	+0.052	+0.037
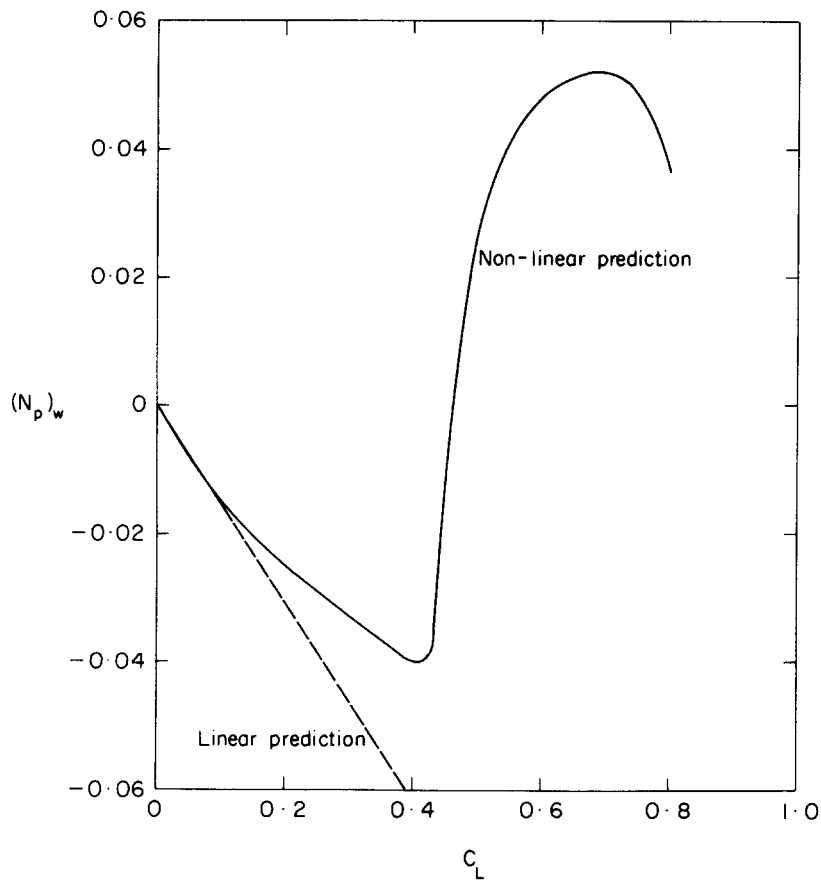
Sketch 8.1   Yawing moment derivative ($A = 2.61, \Lambda_{1/4} = 60°$)
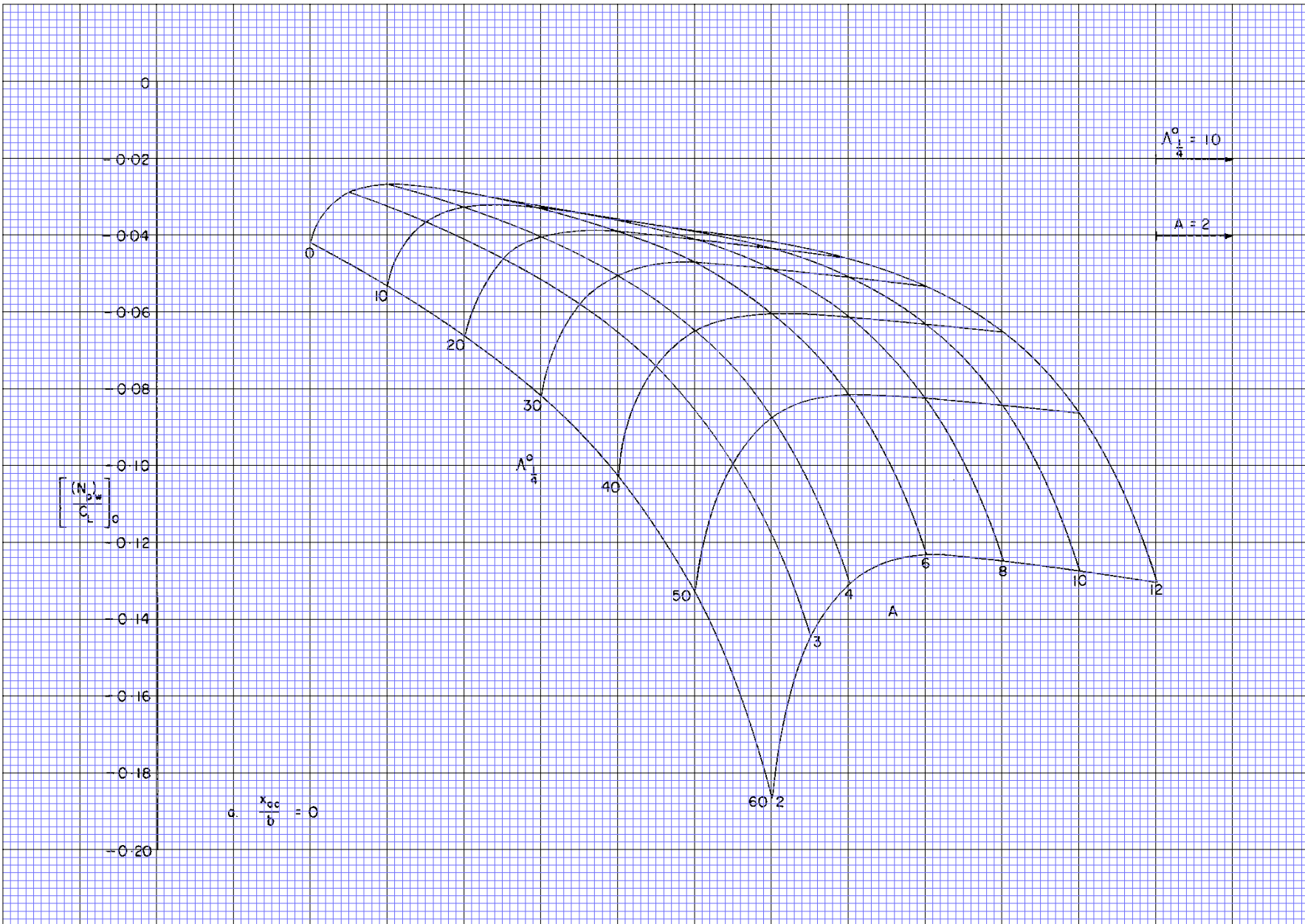
**FIGURE 1 LINEAR CONTRIBUTION TO** $(N_p)_w$

FIGURE 1 (continued)

$$\left[\frac{(N_p)_w}{C_L}\right]_0$$

$$\Lambda^\circ_{\frac{1}{4}}$$

$$\Lambda^\circ_{\frac{1}{4}} = 10$$

$$A = 2$$

$$c. \quad \frac{x_{ac}}{b} = 0.2$$
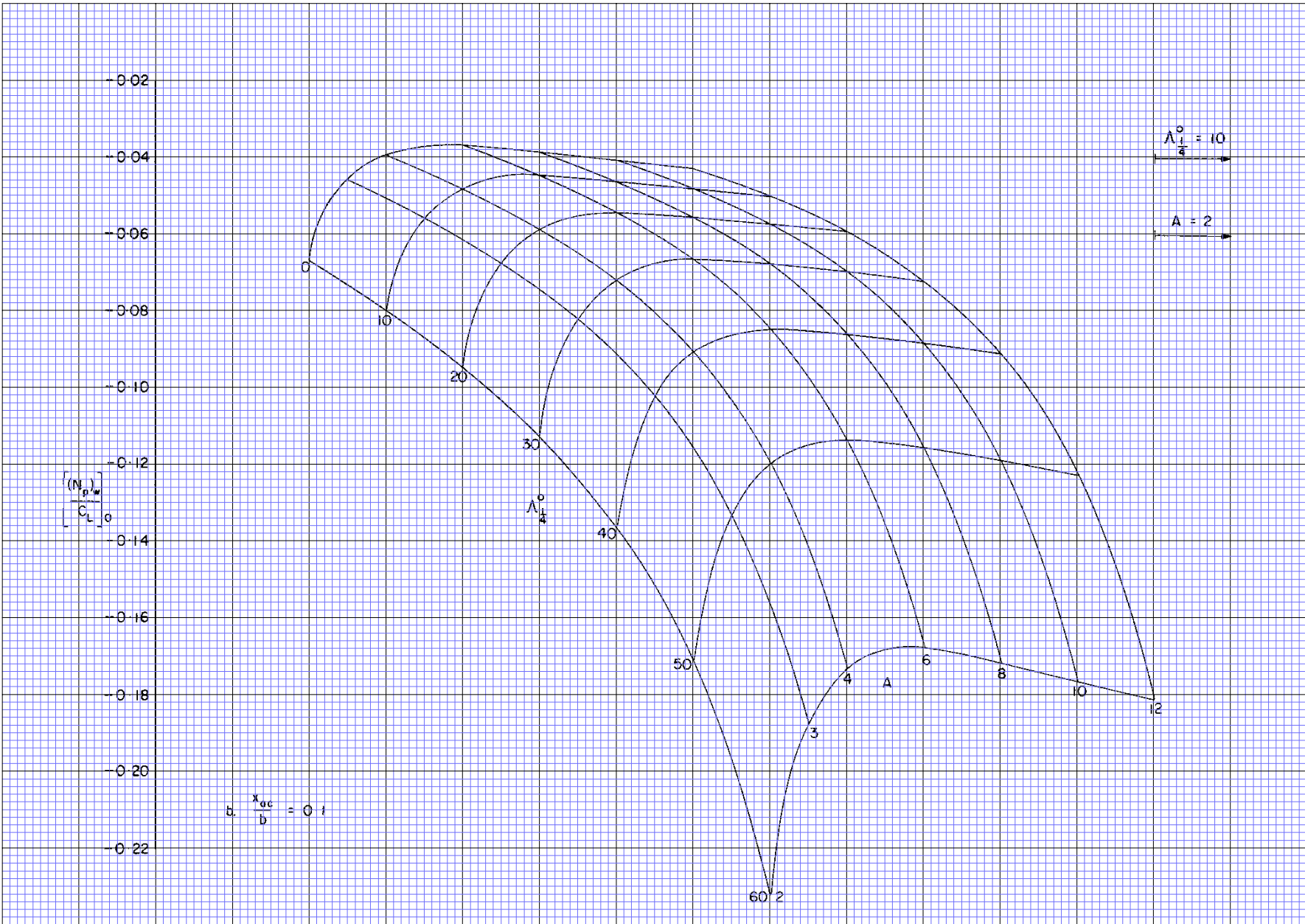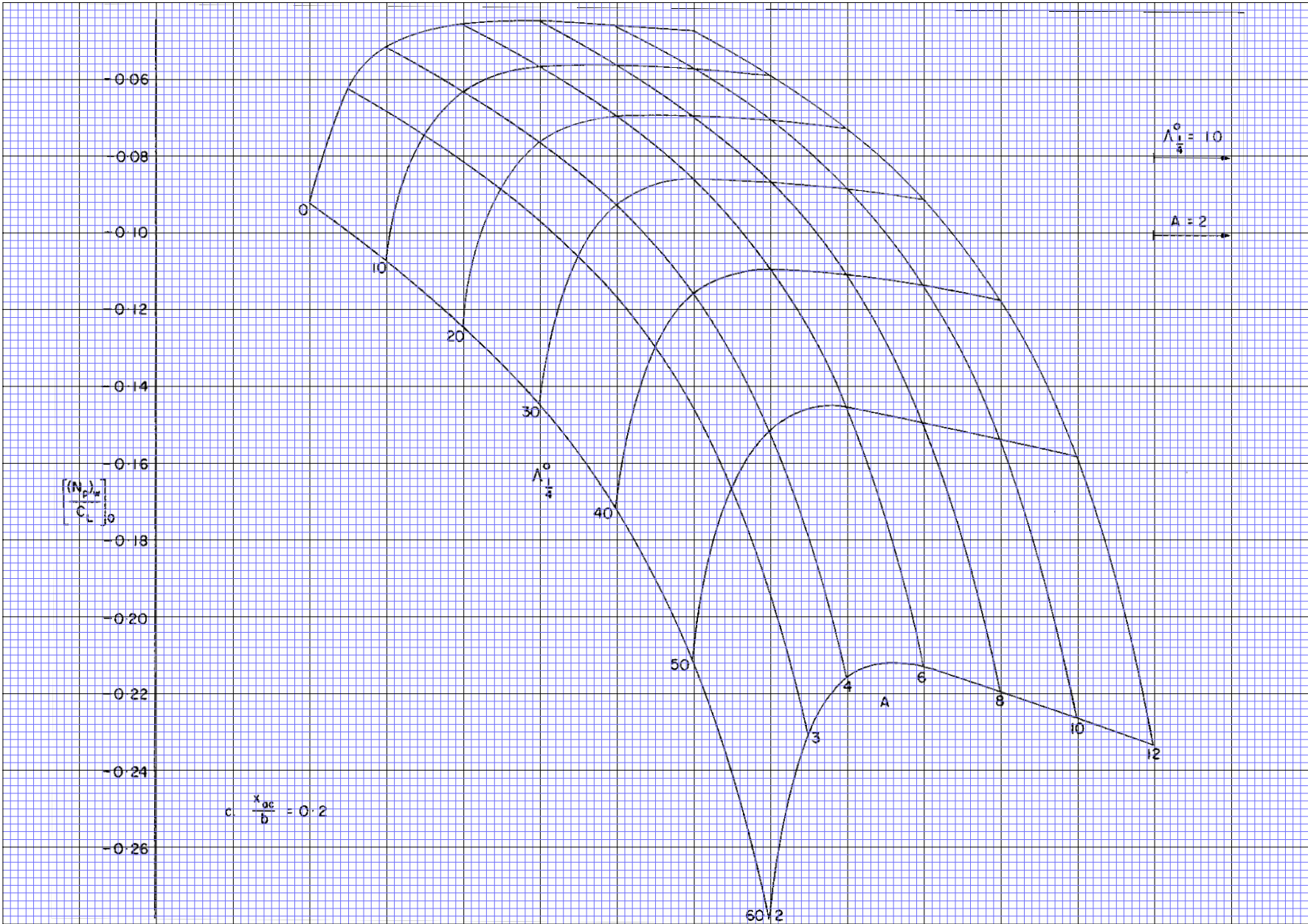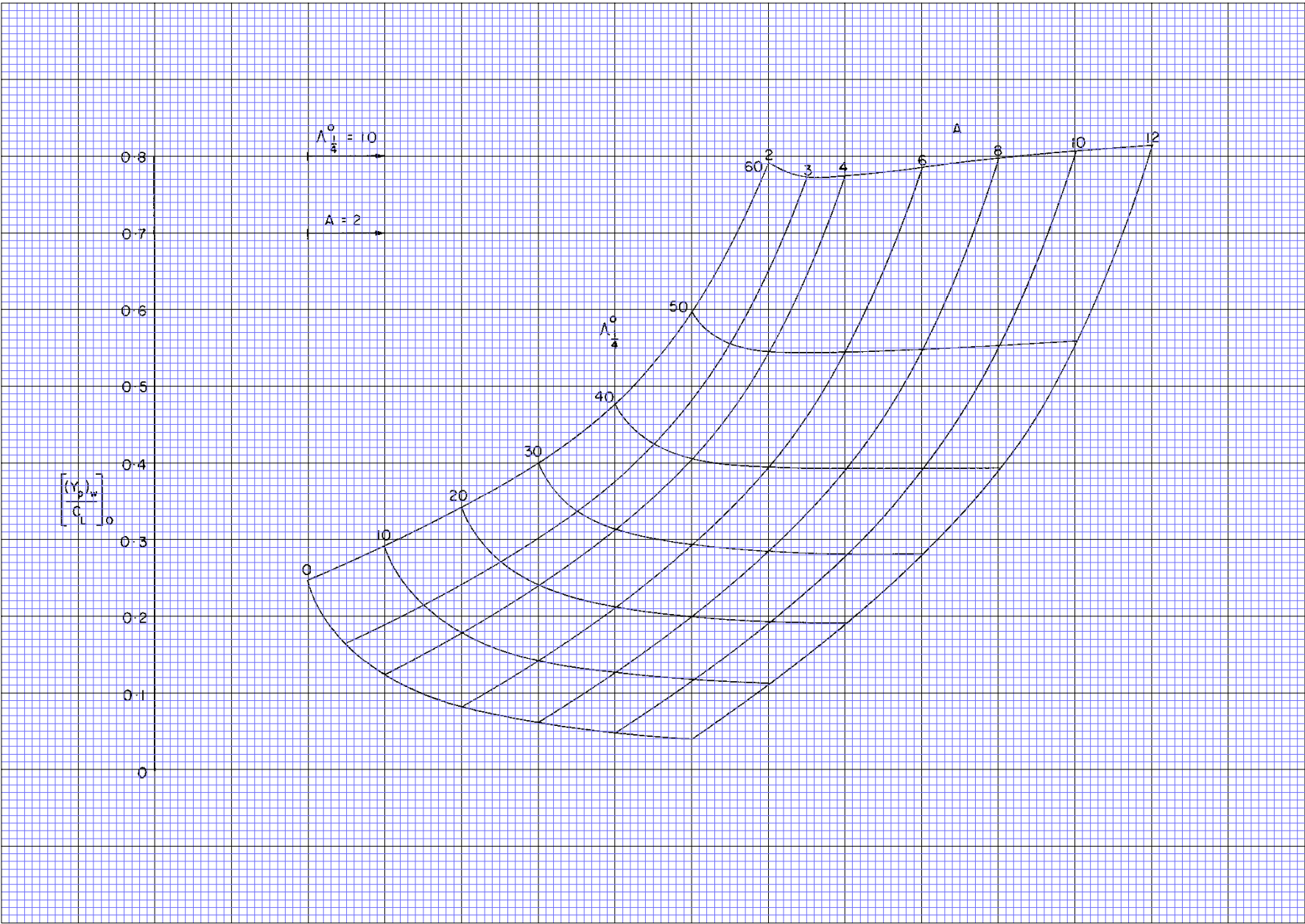
FIGURE 1 (concluded)

FIGURE 2 SIDEFORCE DUE TO ROLL RATE
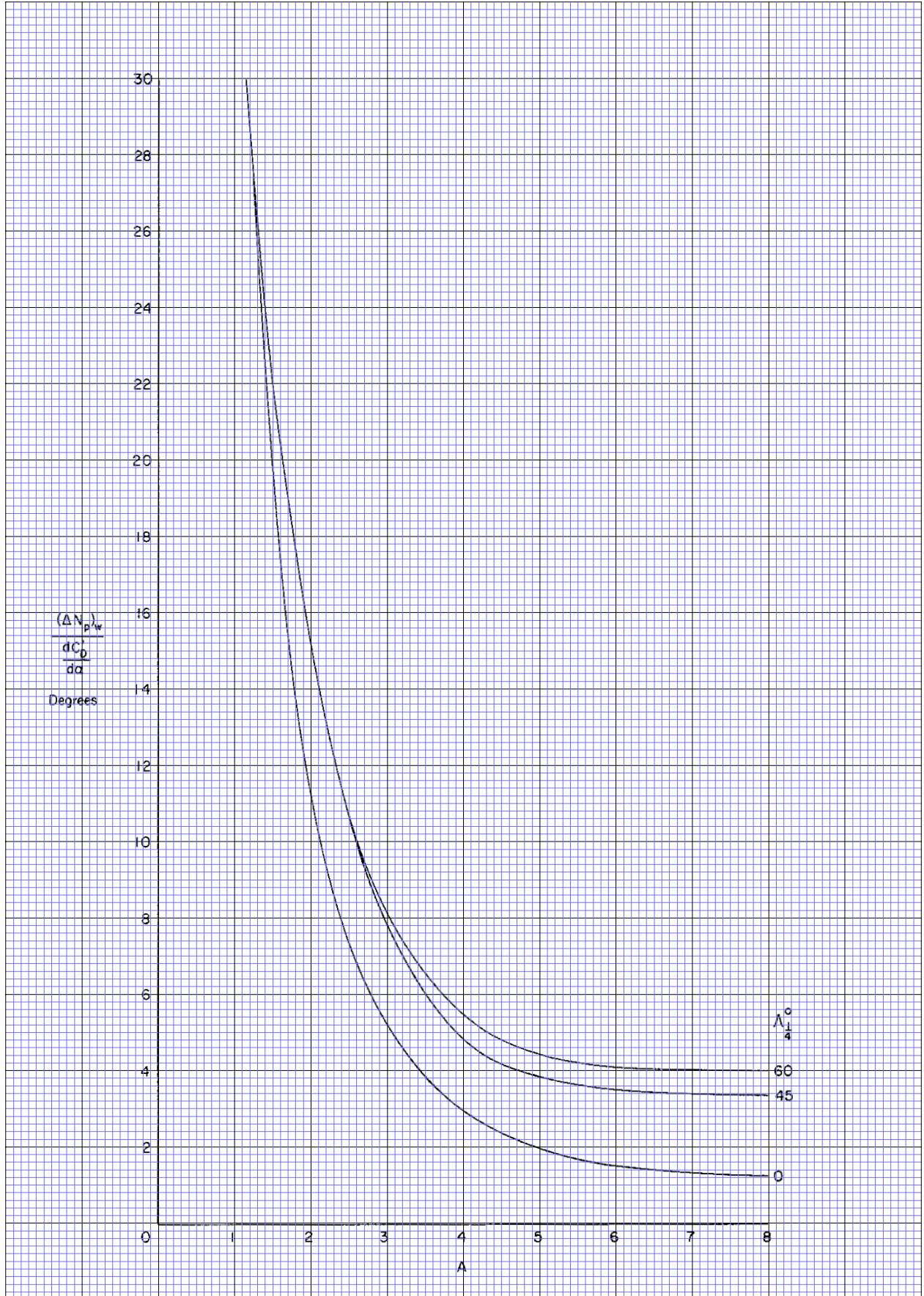
FIGURE 3 VARIATION OF $\dfrac{(\Delta N_p)_w}{\dfrac{dC'_D}{d\alpha}}$ WITH ASPECT RATIO AND SWEEP FOR INCOMPRESSIBLE FLOW
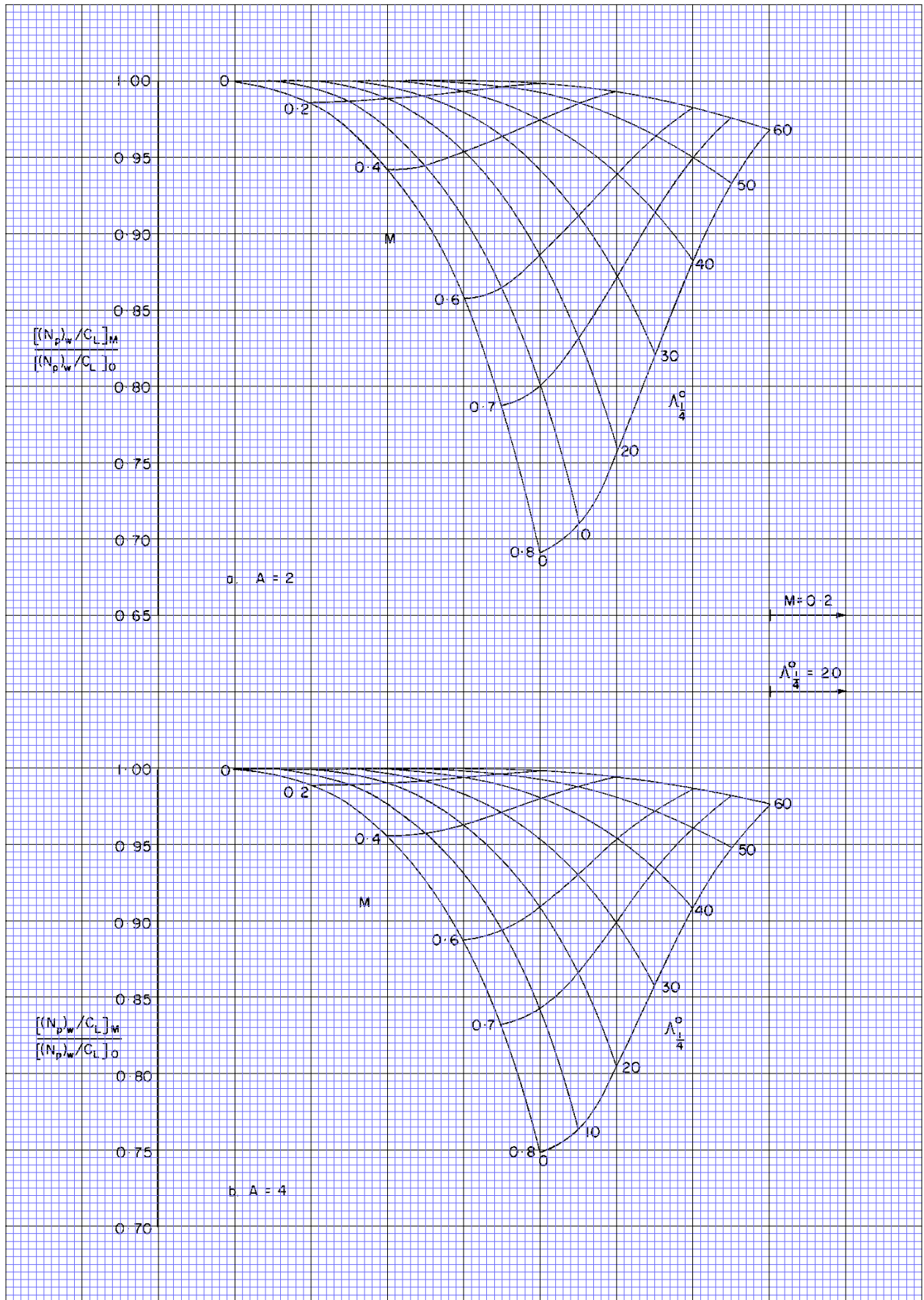
FIGURE 4 CORRECTION FOR THE EFFECT OF COMPRESSIBILITY ON $(N_p)_w$
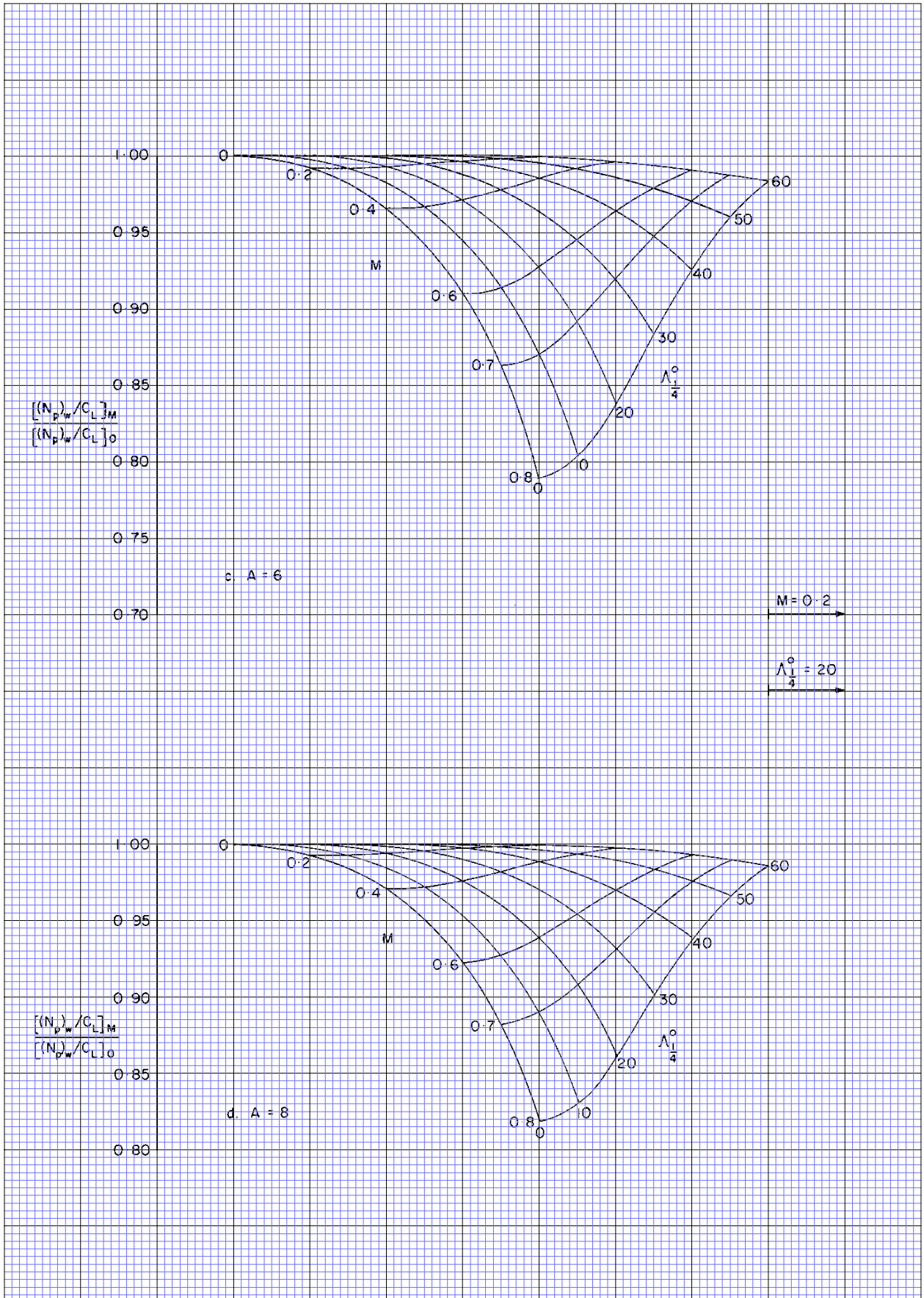
FIGURE 4 (continued)
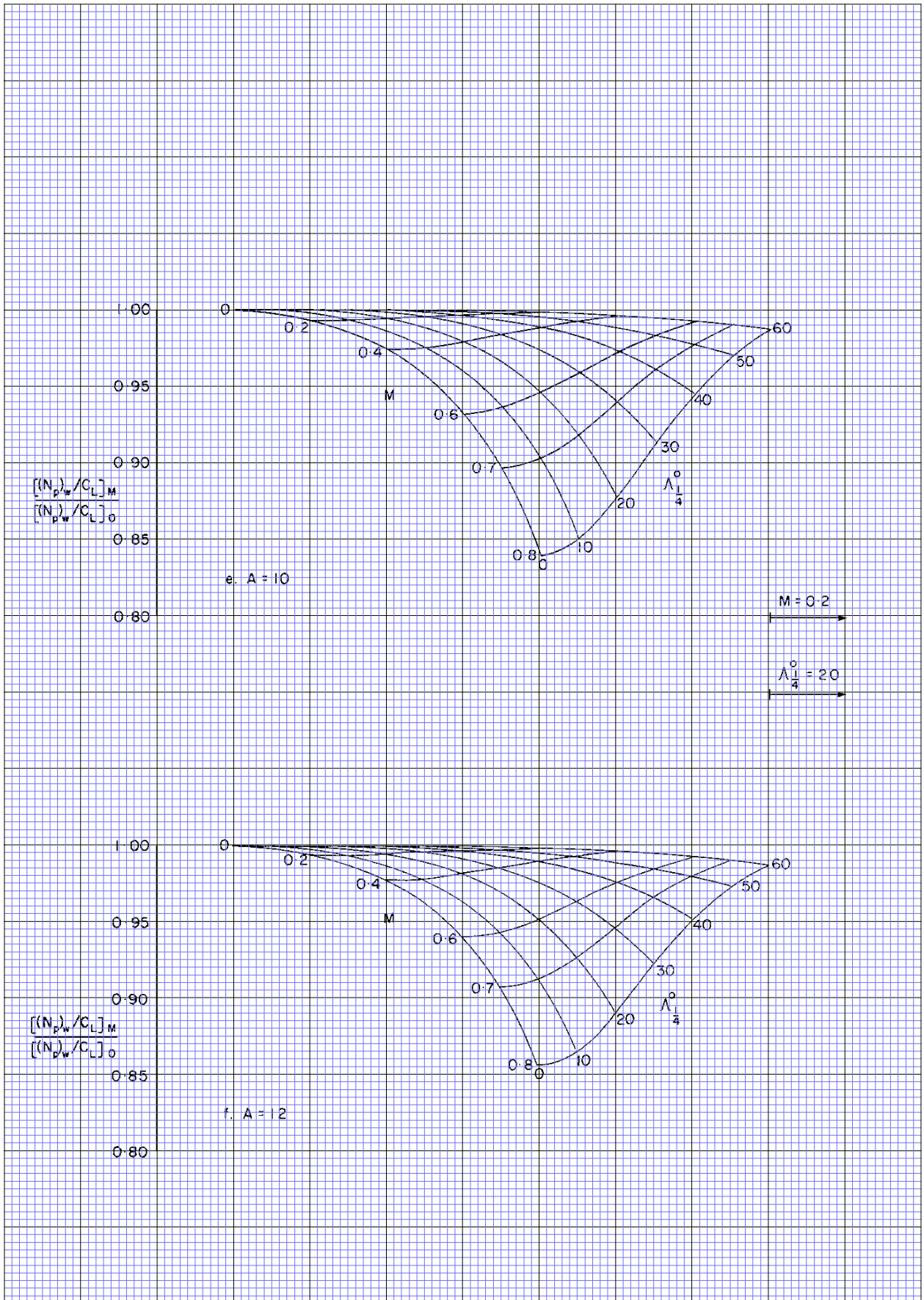
FIGURE 4 (concluded)
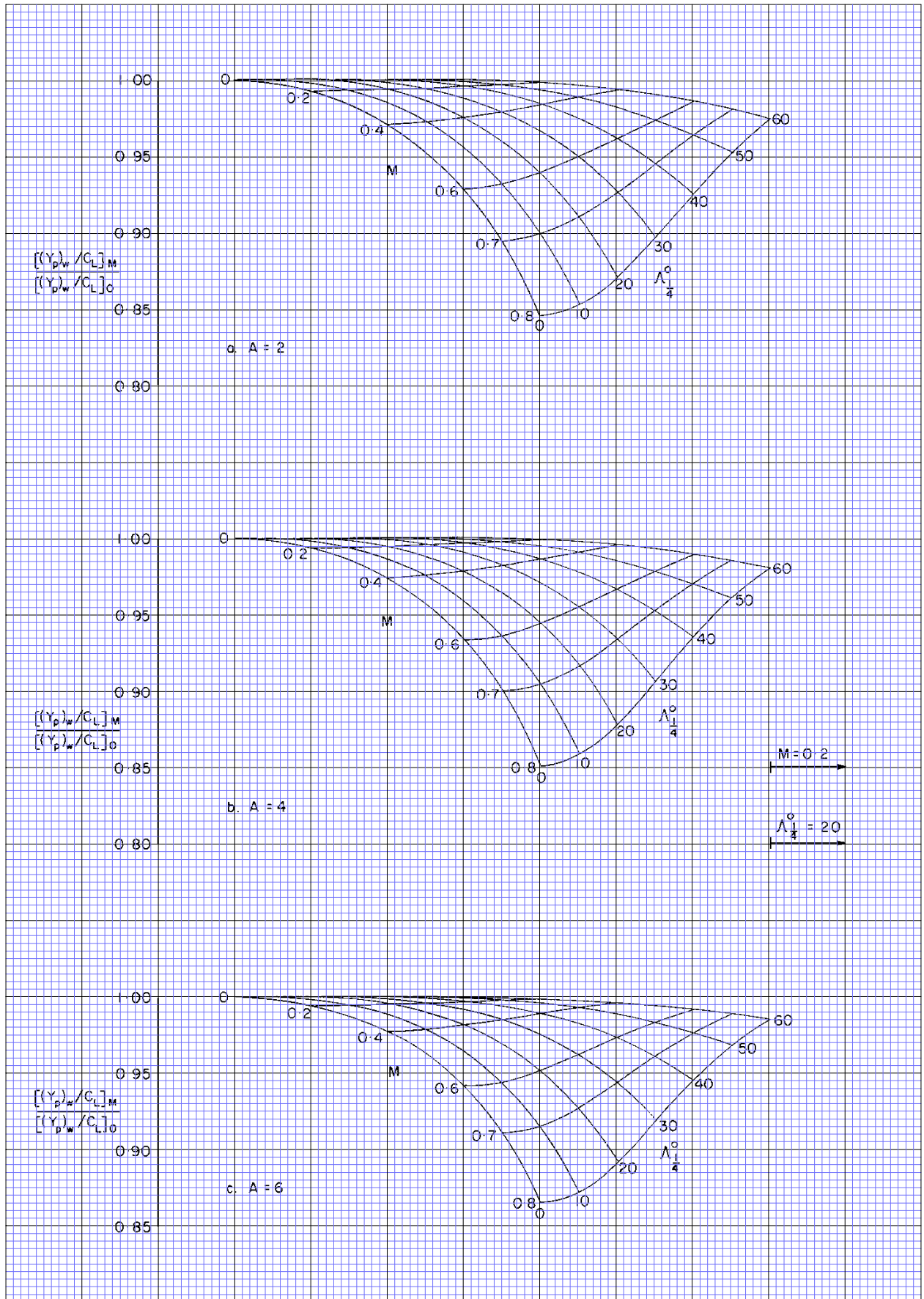
**FIGURE 5 CORRECTION FOR THE EFFECT OF COMPRESSIBILITY ON $(Y_p)_w$**
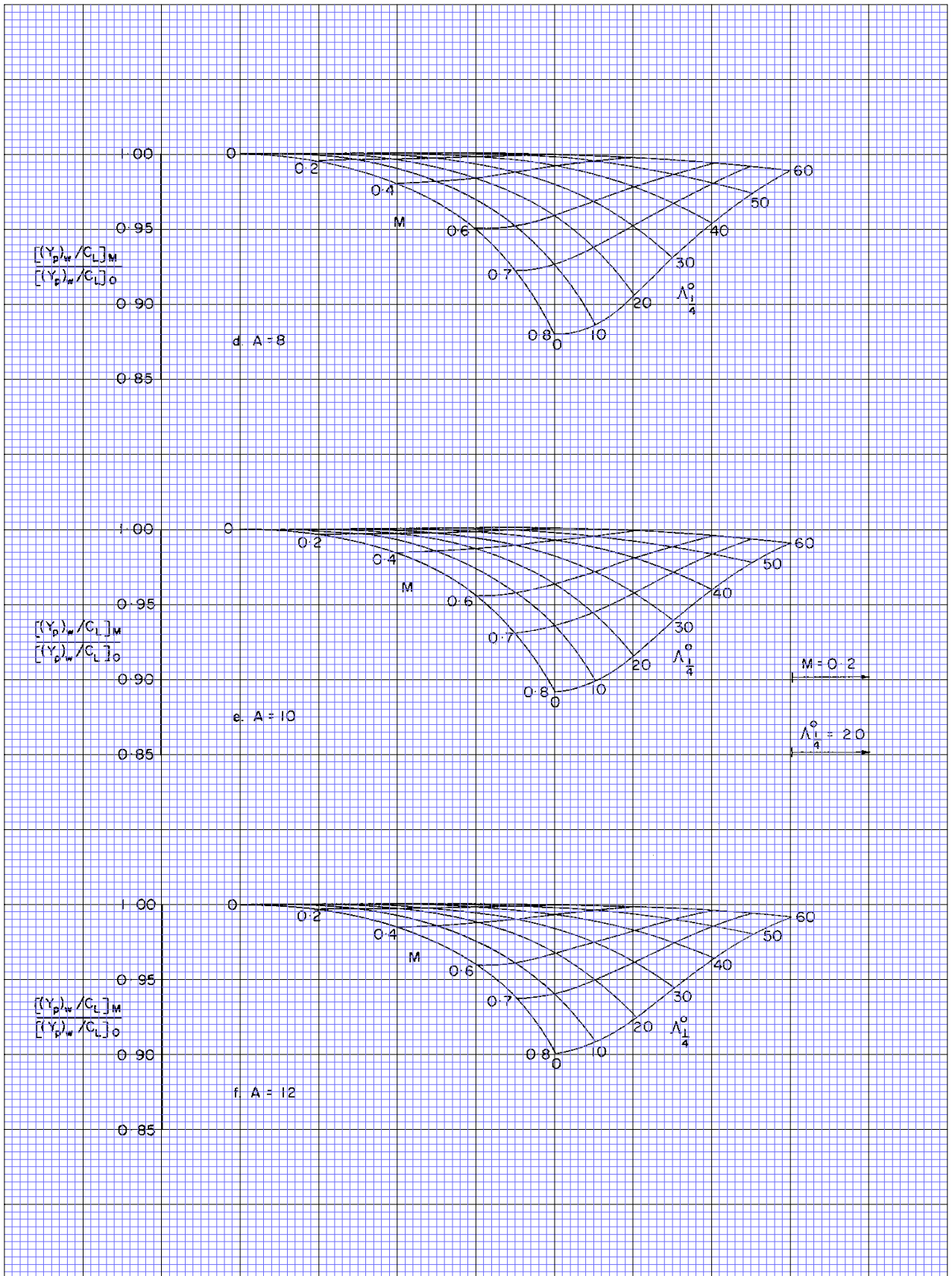
FIGURE 5 (concluded)

THE PREPARATION OF THIS DATA ITEM

The work on this particular Item was monitored and guided by the Aerodynamics Committee which first met in 1942 and now has the following membership:

Chairman
Mr P.K. Jones   – British Aerospace, Manchester Division

Vice-Chairman
Mr J. Weir   – Salford University

Members
Mr D. Bonenfant   – Aérospatiale, Toulouse, France
Mr E.A. Boyd   – Cranfield Institute of Technology
Mr K. Burgin   – Southampton University
Mr E.C. Carter   – Aircraft Research Association
Mr J.R.J. Dovey   – British Aerospace, Warton Division
Dr J.W. Flower   – Bristol University
Mr H.C. Garner   – Royal Aircraft Establishment
Mr A. Hipp   – British Aerospace, Stevenage-Bristol Division
Dr B.L. Hunt[*]   – Northrop Aircraft Group, Hawthorne, Calif., USA
Mr J. Kloos[*]   – Saab-Scania, Linköping, Sweden
Mr J.R.C. Pedersen   – Independent
Mr I.H. Rettie[*]   – Boeing Aerospace Company, Seattle, Wash., USA
Mr F.W. Stanhope   – Rolls-Royce Ltd, Derby
Mr H. Vogel   – British Aerospace, Weybridge-Bristol Division.

[*]   Corresponding Member

The member of staff who undertook the technical work involved in the initial assessment of the available information and the construction and subsequent development of the Item was

Mr L.K. Morris   – Engineer.